A MODEL FOR EVALUATING THE MODAL FREQUENCIES AND ENVIRONMENTAL VIBRATION ENERGY HARVESTING CAPACITY OF RECTANGULAR PIEZOELECTRIC BEAMS

Huiyuan Guo[1], Yujie Zhang[1]
[1]School of Mechanical and Power Engineering, Henan Polytechnic University, Jiaozuo 454000, China
Email: ghy@home.hpu.edu.cn

Abstract - Environmental vibration energy harvesting has received widespread attention recently, but existing research mainly focuses on cantilever beams. The fixing method of the cantilever beams limits its application range. A theoretical model and experimental results of a rectangular piezoelectric beam's modal frequencies and environmental vibration energy harvesting capacity are presented in this study. Accurate evaluation of piezoelectric beams' modal frequencies and energy harvesting capacity is extremely important to monitor and harvest energy from environmental vibrations. This paper establishes a model for the modal frequencies and response of a rectangular piezoelectric beam based on the Euler-Bernoulli beam theory and piezoelectric constitutive equation. In this paper, a fixed-size rectangular piezoelectric beam was selected for verification. The theoretical model was calculated using the modal superposition method. Then, the modal frequencies of piezoelectric beams were simulated using COMSOL, which is a multiphysics simulation software, and compared with theoretical values. Next, the modal frequencies of the piezoelectric beams and the vibration response of the theoretical results were verified through multiple sets of experiments. The experimental results show that the theoretical evaluation error of the modal frequencies of the piezoelectric beams is 1.23%, and the calculation average errors of the output voltage and power of the rectangular piezoelectric beams are 2.7% and 12.3%. The theoretical model effectively predicted the modal frequencies, output voltage, and power of the rectangular piezoelectric beams, demonstrating its potential for monitoring and harvesting environmental vibration energy.

Keywords: Rectangular piezoelectric beams, Dynamic model, Modal frequencies, Vibration energy harvesting capacity, Finite element analysis

1. Introduction

Environmental vibration energy, such as airflow, water waves, and mechanical and human motion vibration energy, is abundant and available. The basic challenge of energy harvesting is how to convert environmental energy into electrical energy effectively. The principle of obtaining energy from environmental vibrations can be roughly divided into four mechanisms: electromagnetic mechanism [1], friction mechanism [2], electrostatic mechanism [3], and piezoelectric mechanism [4-17]. A vibration-based piezoelectric energy harvester is a potential candidate to replace existing power sources, such as batteries which have limited energy storage capacity and lifetime for some applications.

Dhote et al. [4] designed a nonlinear multi-mode broadband piezoelectric vibration energy harvester, and experimental results showed that there were multiple vibration modes at lower frequencies. By adopting a flexible structure design, the bandwidth was widened and the output voltage of the structure was increased. Leland and Wright [5] designed a piezoelectric energy harvester with adjustable resonant frequency. The resonant frequency is related to stiffness, which is determined by the stress applied in the x-direction at both ends, indirectly making the frequency of the structure adjustable. The cantilever beam has a length of 31.7mm, a width of 12.7mm, a centre mass block of 7.1g, and a frequency range of 200Hz to 250Hz, resulting in an output power of 300 μ W and 400 μ Between W. Liu et al. [6] also designed an array-type piezoelectric energy harvester, which uses piezoelectric cantilever beams of different volumes. These cantilever beams are sequentially connected in series to form the structure. Among these, a combination of six cantilever beam arrays, each with a length of 12mm and a width of 5mm, was used, and its operating frequency was measured to be 35.8Hz. Under certain acceleration excitation, the output power can reach 11.6nW.

Song et al. [7] proposed a double-cantilever-beam piezoelectric energy harvester that adopted the width-splitting method and asymmetric mass which achieves harvesting the coupled bending-torsion vibrations. Hao et al. [8] were inspired by soybean and used its structure and nanomaterials to create a bistable piezoelectric harvester, which achieves efficient vibration energy harvesting of three vibration modes through its nonlinear characteristics. Jia et al. [9] studied the detection ability of fine-scale 2-2 connectivity PZT/epoxy piezoelectric fibre composite for high-frequency ultrasonic vibration under the same size, different material volume fractions, and different sizes and volumes, and provided their changing trends. Ma et al. [10] proposed a variable-section circular piezoelectric vibration energy harvester which achieved 0.213mW output power and established its dynamic modal and electromechanical coupling model.

To achieve extremely low-frequency vibration energy collection, Zhou et al. [11] applied the flight mechanism of a dipteran biomimetic structure to a piezoelectric energy harvester and achieved an output power of 0.143mW under 4Hz, 0.7g vibration through the bistable characteristics of the biomimetic structure. Derakhshani et al. [12] proposed a piezoelectric polymer PVDF harvester with a bistable bending beam structure, providing a nonlinear electromechanical coupling model through the Hamiltonian principle and Euler-Bernoulli beam theory, ultimately achieving energy harvesting from low-frequency vibrations under various driving conditions below 30Hz. Jing et al. [13] analysed the vibration problem of piezoelectric cantilever beams with bimodular, functionally graded properties and provided the numerical simulation process. Through numerical simulation and experimental verification, it was concluded that the dual-mode functional grading characteristics have a relatively small impact on the dynamic response of piezoelectric cantilever beams.

Chen et al. [14] designed a cantilever plate energy harvester with two boxes added at two free edges along the fix-free direction and placed one rolling ball in each box. They provided the vibration equation of the system through the Hamilton principle and Hertz contact theory. Through numerical simulation and experiments, it was proven that the structure can achieve high-performance energy collection over a wider operating frequency range by adjusting the position of the ball. Khaje et al. [15] investigated active optimal vibration control of a micro-beam integrated with a piezoelectric actuator and sensor based on modified couple stress and surface stress elasticity theories.

The above research mainly focuses on cantilever beam structures, but cantilever beams are difficult to use due to their fixed methods, so it is necessary to study the performance of piezoelectric beams in a fixed-fixed state. Therefore, a model is proposed to evaluate the modal frequency and environmental vibration energy harvesting capacity of fixed-supported piezoelectric beams. In section 2, the modal frequency of piezoelectric beams was studied through a theoretical model and finite element model. Meanwhile, the model of environmental energy harvesting capacity was conducted and solved. In section 3, multiple experiments were conducted to verify the modal frequency and collection ability of piezoelectric beams. In Section 4, the conclusion of the experimental results is presented.

2. Materials and Methods

To evaluate the modal frequencies and environmental vibration energy harvesting capacity of piezoelectric beams, a theoretical model to solve the modal frequencies and harvesting capacity of piezoelectric beams is conducted in the paper. Meanwhile, a finite element model is used to solve the modal frequencies of the piezoelectric beams.

2.1 Theoretical Mathematical Model

To evaluate the vibration characteristic, vibration response and output voltage of rectangular piezoelectric beams, it is necessary to construct the dynamic model of rectangular piezoelectric beams. Meanwhile, this paper chooses the clamped-clamped beam shown in Figure 1 as the research object. It has a length of L, a width of B, a piezoelectric layer thickness of H_p, and a brass layer thickness of H_b.

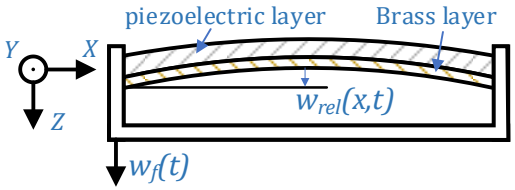

Figure 1: Clamped-clamped piezoelectric beam vibration

Analysing the forces during the beam vibration process, the governing equation of motion for the uniform rectangular beam under undamped vibration can be obtained [16]:

$$\frac{\partial^2 M(x,t)}{\partial x^2} + \rho A \frac{\partial^2 w(x,t)}{\partial t^2} = f(x,t) \quad (1)$$

where *M(x,t) is the Internal bending moment*, ρ is the density of the material, A is the cross-section area,

$f(x,t)$ replaces the extending force, $w(x,t)$ is the transverse displacement of the neutral axis due to the bending. In addition, the transverse displacement $w(x,t)$ can be expressed as:

$$w(x,t) = w_f(t) + w_{rel}(x,t) \tag{2}$$

where $w_{rel}(u,t)$ represents the displacement of the piezoelectric beam relative to the fixed support, and $w_f(t)$ is the foundation displacement of the beam.

To solve the above partial differential equation of motion, it is necessary to first analyse its modal characteristics under free vibration. Ignoring extern forces, the motion equation under free vibration can be expressed as:

$$\frac{\partial^2 M(x,t)}{\partial x^2} + \rho A \frac{\partial^2 w(x,t)}{\partial t^2} = 0 \tag{3}$$

According to the brass and PZT material constitutive equation [17], the stress-strain relationship between the brass layer and piezoelectric layer is determined by

$$\begin{cases} \sigma_x^b = E_b \varepsilon_x^b \\ \sigma_x^p = E_p \varepsilon_x^p - d_{31} V_3^p(t) \end{cases} \tag{4}$$

where σ, E, ε, d_{31} and V_3 are stress, Young's modulus, strain, piezoelectric modulus and electric field strength, superscripts b and p denote the brass layer and the piezoelectric layer.

Through the relationship between internal bending moment and stress, it can obtain the internal bending moment by dividing the cross-sectional area using the above equation as follows:

$$M(x,t) = EI \frac{\partial^2 w(x,t)}{\partial x^2} + \lambda v(t) \tag{5}$$

where v is the voltage on the upper and lower sides of the piezoelectric beam, and λ satisfies the relationship:

$$\lambda = -\frac{E_p B d_{31}}{2}\left(H_b + H_p\right) \tag{6}$$

Because the piezoelectric layer covers the entire beam, using the Heaviside function to solve Equation (5), the internal bending moment turned [18]:

$$M(x,t) = EI \frac{\partial^2 w(x,t)}{\partial x^2} + \lambda v(t)\left[H(x) - H(x-L)\right] \tag{7}$$

Then, substituting Equation (7) into Equation (1) yields, a mechanical equation of motion with an electrical coupling term:

$$\begin{aligned} &EI \frac{\partial^4 w_{rel}(x,t)}{\partial x^4} + \rho A \frac{\partial^2 w_{rel}(x,t)}{\partial t^2} \\ &+\lambda v(t)\left[\frac{d\delta(x)}{dx} - \frac{d\delta(x-L)}{dx}\right] = f(x,t) \end{aligned} \tag{8}$$

where δ represents the Dirac delta function.

On the other hand, to obtain an electrical circuit equation with mechanical coupling term, it must consider the following piezoelectric constitutive relation [17]:

$$D_3 = d_{31}\sigma + \gamma_{33}^S V_3 \tag{9}$$

where D_3 is the electric displacement in the z-direction, γ is the permittivity at constant stress.

Based on the relationship between electric field strength and voltage and the deformation relationship between stress and displacement, it can be concluded that the electric displacement satisfies the following relationship:

$$D_3(t) = -d_{31} E_p h_{po} \frac{\partial^2 w_{rel}(x,t)}{\partial x^2} - \gamma \frac{v(t)}{h_p} \tag{10}$$

where h_{po} is the distance from the centre of the piezoelectric layer to the neutral axis of the beam.

The electric charge accumulated in the piezoelectric layer $Q(t)$ is obtained by integrating the electric displacement for the region of piezoelectric [17], it is represented as:

$$\begin{aligned} Q(t) &= \int D_3 \cdot n dA \\ &= -\int_{x=0}^{L}\left[d_{31} E_p h_{po} B \frac{\partial^2 w_{rel}}{\partial x^2} - \gamma_{33}^S B \frac{v(t)}{H_p}\right] dx \end{aligned} \tag{11}$$

By taking the derivative of time using Equation (11) and multiplying it by the circuitous resistance, the voltage can be obtained as:

$$\begin{aligned} v(t) &= R_L \frac{d\int D_3 \cdot n dA}{dt} \\ &= -R_L \int_{x=0}^{L} d_{31} E_p h_{po} B \frac{\partial^3 w_{rel}}{\partial x^2 \partial t} dx - \frac{\gamma_{33}^S BL}{H_p} \frac{dv(t)}{dt} \end{aligned} \tag{12}$$

By using the modal superposition method, the solution under free vibration of piezoelectric beams can be represented by modal functions and generalized coordinates:

$$w_{rel}(x,t)=\sum_{k=1}^{\infty}W_k(x)q_k(t) \tag{13}$$

where $W_k(x)$ and $q_k(t)$ are mass normalized eigenfunction and the modal coordinate of the clamped-clamped uniform beam of k-order mode.

Substituting Equation (4) into Equation (3), the modal frequencies and modal function of a clamped-clamped beam obtained, which can be expressed as:

$$\omega_k=\beta^2\sqrt{\frac{EI}{mL^4}} \tag{14}$$

$$W_k(x)=\cosh(\beta x)-\cos(\beta x)+\varphi(\sinh(\beta x)-\sin(\beta x)) \tag{15}$$

where constant β and φ can be expressed as:

$$\cos(\beta L)\cosh(\beta L)=1 \tag{16}$$

$$\varphi=-\frac{\sinh(\beta L)+\sin(\beta L)}{\cosh(\beta L)-\cos(\beta L)} \tag{17}$$

For using the modal superposition method, it is assumed that the motion of the beam $w_b=Z_0e^{jwt}$ and the output voltage $v(t)=V_0e^{jwt}$.

Then, substituting Equation (13) into Equation (12), the output voltage of the rectangular piezoelectric beam can be written as:

$$v(t)=\frac{\sum_{k=1}^{\infty}\frac{j\rho AZ_0e^{jwt}\omega_k^3\int_0^L W_k(x)dx}{\omega_k^2-\omega^2-\zeta\omega_k\omega}}{\sum_{k=1}^{\infty}\frac{j\omega_k\lambda W_k'\psi_k}{\omega_k^2-\omega^2-\zeta\omega_k\omega}+\frac{1+j\omega C}{C}} \tag{18}$$

where constant C represents:

$$C=\frac{R_L\gamma_{33}^S BL}{h_p} \tag{19}$$

The voltage output of a rectangular piezoelectric beam under base vibration excitation can be obtained through the above process.

2.2 Finite Element Analysis

This paper takes the piezoelectric beam shown in Figure 2 as the research object.

As shown in Figure 2, the composition of the rectangular piezoelectric beam consists of a brass layer covered with a PZT-5H piezoelectric layer of equal width, with the longer part of the brass layer used for clamping on the base. The surface of the piezoelectric ceramic layer is covered with an extremely thin electrode layer and soldered with wires for connecting external circuits.

This paper uses a simple pure resistance circuit for further research. The two ends of its resistor are connected to the upper and lower sides of the piezoelectric layer. Its size parameters and material parameters are shown in Table 1.

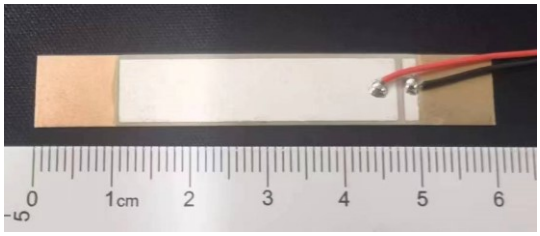

Figure 2: The rectangular piezoelectric beams as research objects

Table 1: The size parameters and materials parameters of the beam

Name	Symbol	Parameter
Length (mm)	L	40
Width (mm)	B	10
Thickness of Brass layer(mm)	H_b	0.35
Thickness of PZT layer(mm)	H_p	0.2
Young's Module of Brass (GPa)	E_b	128
Young's Module of PZT (GPa)	E_p	56
Density of Brass (kg/m^3)	ρ_b	8250
Density of PZT (kg/m^3)	ρ_p	7500
Piezoelectric modulus (C/m^2)	d_{31}	6.6
Permittivity (F/m)	γ_{33}	1433

To better study the vibration characteristics of piezoelectric beams, the finite element software COMSOL Multiphysics 6.1 [19] was used to simulate and analyse the vibration characteristics of the rectangular piezoelectric beam.

At first, use Solid Mechanics (solid) and Electrostatics (es) connected by Multiphysics Piezoelectricity (pze) physics modules of the software to create a study. Then, build the 3D modal of the rectangular piezoelectric beam with length L, width B and two layers for the block geometry. Add the materials Brass and PZT-5H from the materials library and assign them to the corresponding layers separately. Next, add boundary constraints at both ends of the brass layer and grounding constraints to the lower layer of the PZT layer. The other end of the resistor circuit with one side grounded is connected to the upper end of the piezoelectric layer. At last, create an eigenfrequency study to calculate the modal frequencies of the rectangular piezoelectric beam. The first three modal frequencies and modes are shown in Figures 3 to 5.

According to Figures 3 to 5, it can be seen that the finite element analysis of the beam obtained the modal frequencies of the beam and their corresponding modal functions at the frequencies. Compared with the modal frequencies calculated by Equation 14 in the previous theory, the results are shown in Table 2.

According to Table 2, the theoretical calculation results are close to the finite element analysis results, but to better verify the reliability of the results, further verification is needed through experiments.

Table 2. Finite element and theoretical results of the first three modal frequencies

Order	FEA	Theoretical	Error
1-order	1187.7	1172.0	1.32%
2-order	3210.0	3169.2	1.27%
3-order	6412.5	6341.3	1.11%

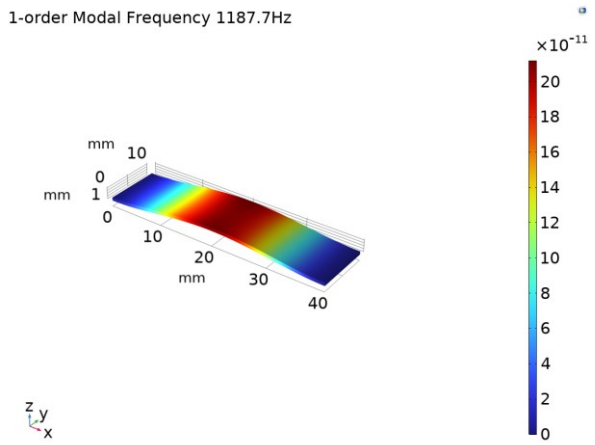

Figure 3: The 1-order modal frequency and modal function

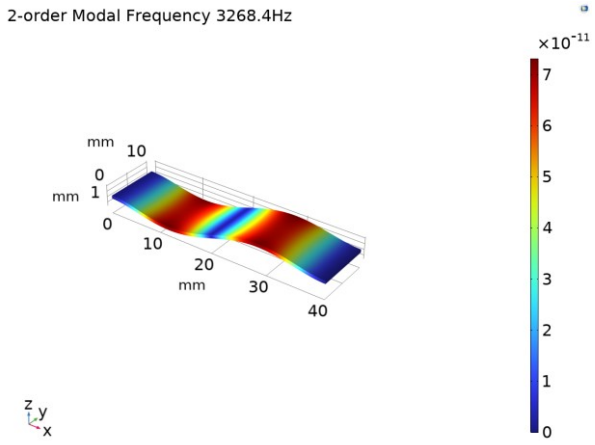

Figure 4: The 2-order modal frequency and modal function

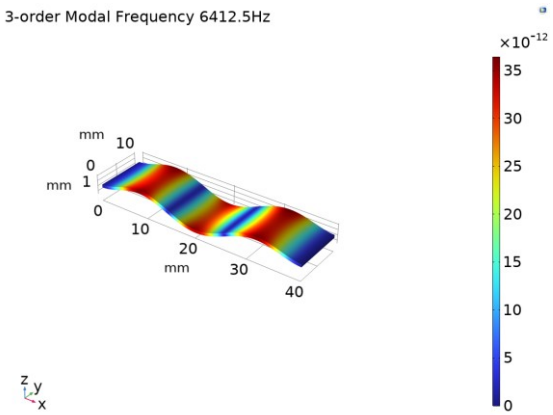

Figure 5: The 3-order modal frequency and modal function

3. Experiment and Result

To verify the feasibility and accuracy of the proposed model and vibration characteristics of the beam, several experiments are carried out.

An experimental platform is established and contains a function generator (RIGOL DG4102), a power amplifier (Aigtek ATA-3080), a shaker (SA-JZ002), an oscilloscope (GW GDS-2204B), an acceleration sensor (DH 1A803E), a data acquisition system (DH5981), a data acquisition software (DHDAS) and a computer, then, the rectangular piezoelectric beam is fixed on the vibration platform. which is shown in Figure 6. The experimental data are processed using ORIGIN 2018 and EXCEL 2021.

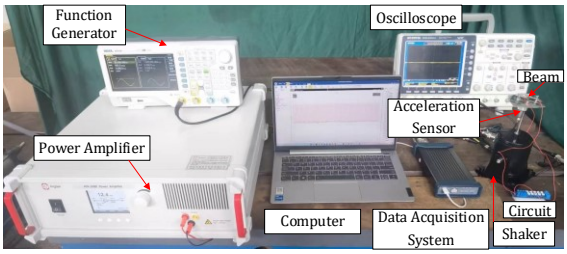

Figure 6. The rectangular piezoelectric beam test platform

In experiments, the function generator generates a fixed-frequency low-voltage sine signal, whose voltage is amplified by a power amplifier. The amplified electrical signal is input to the shaker. Then, a fixed frequency excitation is obtained, which is exerted on the rectangular piezoelectric beam. Meanwhile, the response of the piezoelectric beam is obtained by the acceleration sensor fixed on the test platform. In this process, vibration experiments are conducted under the excited acceleration of 0.1g, 0.2g, 0.3g and 0.4g (g is gravity acceleration) to verify the output voltage of the beam.

To verify the fundamental frequency of the beam, the function generator was adjusted in the frequency range of 1100-1200Hz, and the vibration acceleration of the vibrator was controlled to be the same at different frequencies through the acceleration sensor. The beam excited by the shaker under different excitations of 0.1g, 0.2g, 0.3g and 0.4g, and the relationship between frequency and output voltage is shown in Figure 7.

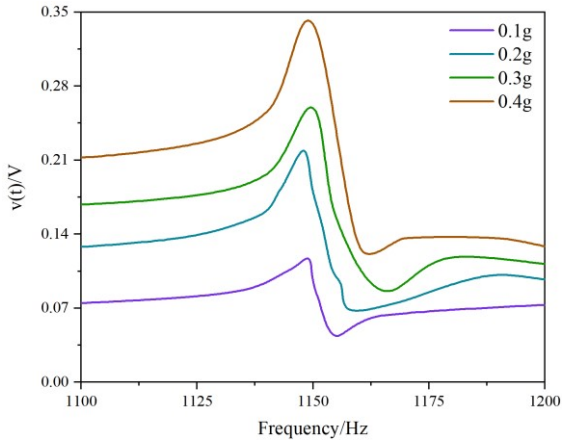

Figure 7. Relationship of frequency and output voltage of piezoelectric beam under various excitations

From Figure 7, it can be found that the output voltages of the piezoelectric beam increase with the increase of the external excitation. Specifically, the output voltages of the piezoelectric beam stably change with the increase of frequency under external excitation 0.1g and the maximum peak output voltage 116.68mV at the resonant frequency 1148Hz. Subsequently, the output voltages sharply decline to 42mV, then, they arise to a stable state. The same change trend can be seen at the other external excitations of 0.2g, 0.3g and 0.4g. Then, when the excitation acceleration reaches 0.2g, the piezoelectric beam produces the maximum peak output voltage at the same frequency of 1148Hz, which reaches 218.90mV. Likewise, when the excitation is further increased to 0.3g and 0.4g, the piezoelectric beam also produces the maximum output voltage at the frequency of 1148Hz, and the output voltages increase to 259.21mV and 338.59mV, respectively. At the same time, according to the above results, it can be seen that the error between the measured modal frequency of the rectangular piezoelectric beam and that calculated in Table 2 is 2.10%. In addition, we found that when the frequency exceeds 1148Hz, the output voltages decline greatly. The reason for this is an anti-phase synchronous motion is generated around the first-order natural frequency, which leads to a low bending amplitude and consequently, the output voltage reduces significantly. Conversely, the output voltages change stably when the frequencies are away from the modal frequency of 1148Hz.

To verify the output voltage of the piezoelectric beam under different excitation accelerations, the output voltage of the piezoelectric beam under different accelerations was tested using first-order modal frequency 1148Hz, and the results are shown in Figure 8.

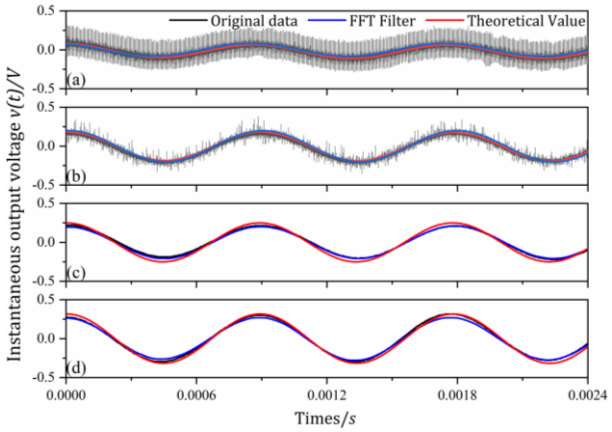

Figure 8. Instantaneous output voltage under 1148Hz (a) 0.1g, (b) 0.2g, (c) 0.3g, (d) 0.4g

From Figure 8, it can be seen that the output voltage of the beam is approximately a harmonic function, and the calculated values agree well with the measured values. Concretely, it can be found that the measured output voltages are affected by electrical noise, especially under small excitation. Under this circumstance, the 50-5000Hz band-pass FFT filtering is applied to avoid the effect of current noise and high-frequency electrical noise, which has an obvious effect on the output response under small external excitation. Further, under an external excitation of 0.1g, the measured value, FFT band-pass filtering results and calculation results are described in Figure 8(a), and the difference between the experimental results and the theoretical results is 12%, which is affected by the measured environment. For an external excitation under 0.2g, the noise effect is smaller and the error is 6.1%, which is seen in Figure 8(b). Similarly, from Figure 8(c) and Figure 8(d), under external excitations of 0.3g and 0.4g, the noise is small, the effect of the noise can be ignored, and the errors between the experimental results and the calculated results are 2.0% and 2.2%, respectively. In short, under different excitations, the proposed model can obtain better accuracy.

To study the relationship between the output voltage and vibration acceleration, the average peak-to-peak voltage of the experimental values is considered. The results are shown in Figure 9.

For output voltage, the output voltage of the beam under different external excitations is shown in Figure 9. It can be seen that the output voltage grows greatly with the increase of excitation, and the output voltage under an excitation of 0.2g is 2.01

times than that under an excitation of 0.1*g*, similarly, the output voltage under an excitation of 0.3*g* is 3.37 times than that under an excitation of 0.1g and the output voltage under an excitation of 0.4*g* is 4.11 times than that under an excitation of 0.1*g*. The overall trend of output voltage shows linear growth, and the calculated values agree well with the measured values. Specifically, compared with the theoretical results, the errors in the output voltage are 1.5%, 1.1%, 5.3%, and 1.7% for external excitations of 0.1*g*, 0.2*g*, 0.3*g*, and 0.4*g*, respectively. It can be seen that the theoretical results for a piezoelectric beam over a long period are more accurate than those calculated in a short period.

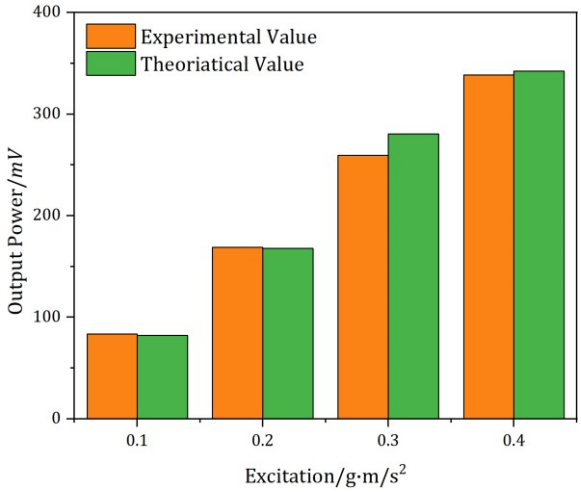

Figure 9. Average output voltages under different excitations

Due to the internal resistance of piezoelectric beams, their output voltage is correlated with the load resistance. Therefore, it is necessary to conduct experiments on the output voltage of piezoelectric beams under different load resistances, and the results are shown in the figure. To verify the output voltage of the beam under different load resistances, the constant frequency 1148Hz and external excitation 0.4*g* are chosen for obtaining the relationship between output voltage and resistance, which is shown in Figure 10.

From Figure 10, it can be found that the theoretical results of the output voltage agree well with the experimental results, the maximum and the minimum errors are 12.31% and 0.17%, respectively. And the average error is 2.7%. In addition, under a small resistance of 0-100kΩ, the predicted accuracy is very high, and the output voltage increases sharply. Then, with the growth of resistance, output voltages improve and reach a fixed value after 250kΩ. The reasons for this are that the series voltage division formula occurs, and the output voltage at both ends of the load resistor is approximately equal to $R_L/(R_L+R_0)*V_0$, where V_0 is the ideal output voltage. According to the output properties of the beam, the output voltages should be large for monitoring the vibration signal in environmental vibration, at the same time, the load resistance exceeding 150kΩ is selected for application.

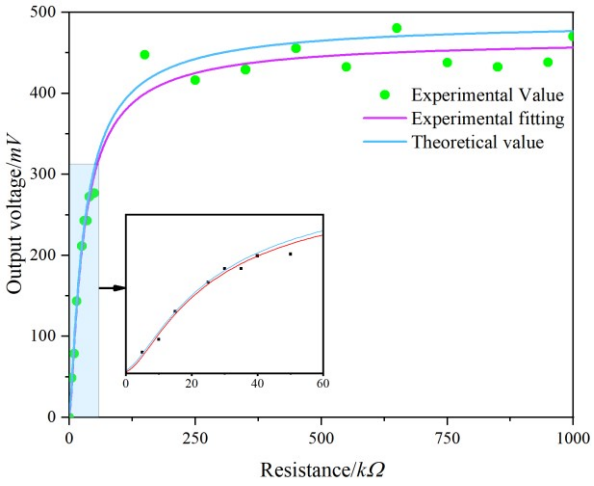

Figure 10. Output voltage under different resistances

On the other hand, many electrical devices require sufficient power supply, so the relationship between output power and load resistance of the beam needs to be studied. Due to the internal resistance of piezoelectric beams, the relationship between their maximum output power and load resistance and voltage may vary. This means that the load resistance used for maximum output voltage and maximum output power is not the same.

Consequently, to validate the output power of the rectangular piezoelectric beam in environmental vibration, a constant frequency of 1148Hz and an external excitation of 0.4*g* were selected for obtaining the relationship between output power and resistance, as shown in Figure 11.

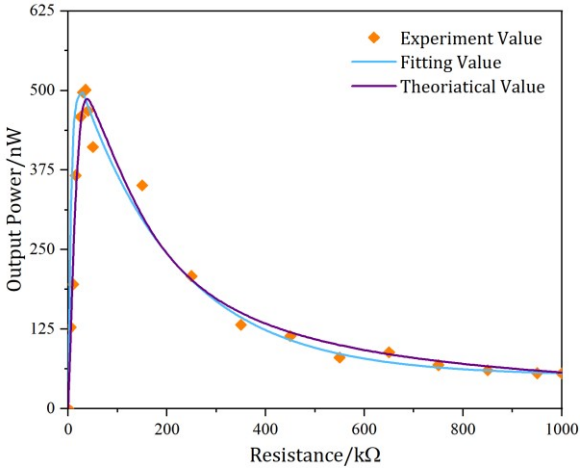

Figure 11. Output power under different resistances

From Figure 11, it can be seen the output power sharply increases under 0-40kΩ and then decreases

under 40-800kΩ, until it reaches a stable state under 1000kΩ, which is determined by the relationship of load residence and internal resistance, and when the load resistance is equal to the internal resistance, the maximum power output can be achieved. In experiments, the results are shown that the maximum power output of the beam reaches 496.92nW at 30kΩ, then, the output power slowly decreases and is close to 56.77nW. Next, from Figure 11, it is also found that a maximum error of the theoretical value and the experimental value is 23.46% at 550kΩ, a minimum error is 0.85% at 200kΩ, and an average error is 12.3%, which signifies that the proposed model is effective in predicting the properties of the beam.

4. Conclusions

This paper investigates the modal frequency and environmental vibration energy harvesting capacity of a rectangular piezoelectric beam with a length of 40mm and a width of 10mm, a bronze layer thickness of 0.35 mm and a piezoelectric layer thickness of 0.2 mm, under a fixed support state. In this paper, a theoretical model of the output voltage of a rectangular piezoelectric beam under external excitation was constructed using beam theory and the piezoelectric constitutive equations.

To verify the theoretical feasibility of the piezoelectric beam, COMSOL was first used to simulate and verify the modal frequency of the beam. Then, multiple sets of experiments were conducted and compared with the theoretical values. The experimental results have verified the accuracy of theoretical calculations and demonstrated the application characteristics of piezoelectric beams.

The following are the key summary and findings of the study:

(1) The comparison between the theoretical model and experimental results in the paper shows that the calculation error for modal frequencies is 1.23%, the calculation error for output voltage is 2.7%, and the calculation error for output power is 12.3%. The theoretical model can provide a method for solving the modal frequencies, output voltage, and output power of piezoelectric fixed supported beams with similar structures.

(2) The first modal frequency of the piezoelectric beam is 1148Hz, and the output voltage of the piezoelectric beam is maximum when excited at its modal frequency.

(3) With the increase of environmental vibration acceleration, the output voltage of the piezoelectric beam increases linearly, and its output voltage frequency is the same as the excitation.

(4) The output voltage of a piezoelectric beam is related to the load resistance. As the load resistance increases, the output voltage first increases sharply and gradually tends to a stable value after 250kΩ.

(5) The output power of piezoelectric beams is also related to load resistance. After reaching its maximum value in linear growth, it rapidly decreases, and gradually approaches a stable value.

References

[1] Wang Y, Wang P, Li S, Gao M, Ouyang H, He Q, Wang P. (2022). An electromagnetic vibration energy harvester using a magnet-array-based vibration-to-rotation conversion mechanism. Energy Conversion and Management 253: 115146. doi: 10.1016/j.enconman.2021.115146.

[2] Wang K, Zhou J, Ouyang H, Chang Y, Xu D. (2021). A dual quasi-zero-stiffness sliding-mode triboelectric nanogenerator for harvesting ultralow-low frequency vibration energy. Mechanical Systems and Signal Processing 151: 107368. doi: 10.1016/j.ymssp.2020.107368.

[3] Sokolov A, Galayko D, Basset P, Blokhina E. (2023). On the frequency up-conversion mechanism due to a soft stopper by the example of an electrostatic kinetic energy harvester. Journal of Intelligent Material Systems and Structures 34(6): 696-705. doi: 10.1177/1045389X221109258.

[4] Dhote S, Zu J, Yang Z. (2015). A nonlinear multi-mode wide band piezoelectric vibration-based energy harvester using compliant ortho planar spring. Applied Physics Letters, Volume 106, Issue 16, Pp:1291, 2015. doi: 10.1016/j.ijmecsci.2017.11.012

[5] Leland E S, Wright P K. (2006). Resonance tuning of piezoelectric vibration energy scavenging generators using compressive axial preload. Smart Materials & Structures, Volume 15, Issue 5, Pp: 1413-1420, 2006. doi: 10.1088/0964-1726/15/5/030

[6] Liu H, Lee C, Kobayashi T, et al. (2011). Investigation of Piezoelectric MEMS-based Wideband Energy Harvesting System with Assembled Frequency-up-conversion Mechanism. Procedia Engineering, Volume 25, Issue 35, pp: 725-728, 2011. doi: https://doi.org/10.1016/j.proeng.2011.12.179

[7] Song J, Sun G, Zeng X, Li X, Bai Q, Zheng X. (2022). Piezoelectric energy harvester with double cantilever beam undergoing coupled bending-torsion vibrations by width-splitting method. Scientific Reports, Volume 12 Issue 1, 2022. doi: 10.1038/s41598-021-04476-1.

[8] Hao F, Wang B, Wang X, Tang T, Li Y, Yang Z, Lu J. (2022). Soybean-inspired nanomaterial-based broadband piezoelectric energy harvester with local bistability. Nano Energy 103: 107823. doi: 10.1016/j.nanoen.2022.107823.

[9] Jia H, Li H, Lin B, Hu Y, Peng L, Xu D, Cheng X. (2021). Fine scale 2-2 connectivity PZT/epoxy piezoelectric fiber composite for high frequency ultrasonic application. Sensors and Actuators A: Physical 324: 112672. doi: 10.1016/j.sna.2021.112672.

[10] Ma T, Ding Y, Wu X, Chen N, Yin M. (2021). Research on piezoelectric vibration energy harvester with variable section circular beam. Journal of Low Frequency Noise, Vibration and Active Control 40(2): 753-771. doi: 10.1177/1461348420918408.

[11] Zhou J, Zhao X, Wang K, Chang Y, Xu D, Wen G. (2021). Bio-inspired bistable piezoelectric vibration energy harvester: Design and experimental investigation. Energy 228: 120595. doi: 10.1016/j.energy.2021.120595.

[12] Derakhshani M, Momenzadeh N, Berfield TA. (2021). Analytical and experimental study of a clamped-clamped, bistable buckled beam low-frequency PVDF vibration energy harvester. Journal of Sound and Vibration 497: 115937. doi: 10.1016/j.jsv.2021.115937.

[13] Jing H, He X, Du D, Peng D, Sun J. (2020). Vibration Analysis of Piezoelectric Cantilever Beams with Bimodular Functionally-Graded Properties. Applied Sciences 10(16): 5557. doi: 10.3390/app10165557.

[14] Lihua C, Jiangtao X, Shiqing P, Liqi C. (2020). Study on cantilever piezoelectric energy harvester with tunable function. Smart Materials and Structures 29(7): 75001. doi: 10.1088/1361-665X/ab859f.

[15] Khaje Khabaz M, Eftekhari SA, Hashemian M, Toghraie D. (2020). Optimal vibration control of multi-layer micro-beams actuated by piezoelectric layer based on modified couple stress and surface stress elasticity theories. Physica A: Statistical Mechanics and its Applications 546: 123998. doi: 10.1016/j.physa.2019.123998.

[16] Rao SS. (2011) Mechanical Vibrations Fifth Edition. New York: Prentice Hall. ISBN 978-0-13-212819-3

[17] Jalili N. (2010) Piezoelectric-Based Vibration Control. New York: Springer Science+Business Media. ISBN 978-1-4419-0069-2

[18] Muthalif AGA, Nordin NHD (2015) Optimal piezoelectric beam shape for single and broadband vibration energy harvesting: Modeling, simulation and experimental results. Mechanical Systems and Signal Processing 54-55: 417-426. doi: 10.1016/j.ymssp.2014.07.014.

[19] COMSOL (2024) Shear-actuated beam: a static analysis: www.comsol.com/model/piezoelectric-shear-actuated-beam-24 [Access:9/5/2024].